PLOS ONE

RESEARCH ARTICLE

CSB ablation induced apoptosis is mediated by increased endoplasmic reticulum stress response

Manuela Caputo[1], Alessio Balzerano[1], Ivan Arisi[2], Mara D'Onofrio[2], Rossella Brandi[2], Silvia Bongiorni[1], Stefano Brancorsini[3], Mattia Frontini[4,5,6], Luca Proietti-De-Santis[1]*

1 Unit of Molecular Genetics of Aging—Department of Ecology and Biology—University of Tuscia, Viterbo, Italy, **2** Genomics Facility, European Brain Research Institute (EBRI) "Rita Levi-Montalcini", Rome, Italy, **3** Department of Experimental Medicine—Section of Terni, University of Perugia, Terni, Italy, **4** Department of Haematology, University of Cambridge, Cambridge Biomedical Campus, Cambridge, United Kingdom, **5** National Health Service (NHS) Blood and Transplant, Cambridge Biomedical Campus, Cambridge, United Kingdom, **6** British Heart Foundation Centre of Excellence, University of Cambridge, Cambridge Biomedical Campus, Cambridge, United Kingdom

* proietti@unitus.it

Citation: Caputo M, Balzerano A, Arisi I, D'Onofrio M, Brandi R, Bongiorni S, et al. (2017) CSB ablation induced apoptosis is mediated by increased endoplasmic reticulum stress response. PLoS ONE 12(3): e0172399. doi:10.1371/journal.pone.0172399

Editor: Salvatore V Pizzo, Duke University School of Medicine, UNITED STATES

Received: June 22, 2016

Accepted: February 3, 2017

Published: March 2, 2017

Data Availability Statement: All relevant data are within the paper and its Supporting Information files.

Funding: This work was supported by grants from AIRC (IG13074), Telethon (GGP11176), FP7 European Collaborative Project PAINCAGE (603191) and Italian Research Council (EBRI-CNR 2015-2017).

Competing interests: The authors have declared that no competing interests exist.

Abstract

The DNA repair protein Cockayne syndrome group B (CSB) has been recently identified as a promising anticancer target. Suppression, by antisense technology, of this protein causes devastating effects on tumor cells viability, through a massive induction of apoptosis, while being non-toxic to non-transformed cells. To gain insights into the mechanisms underlying the pro-apoptotic effects observed after CSB ablation, global gene expression patterns were determined, to identify genes that were significantly differentially regulated as a function of CSB expression. Our findings revealed that response to endoplasmic reticulum stress and response to unfolded proteins were ranked top amongst the cellular processes affected by CSB suppression. The major components of the endoplasmic reticulum stress-mediated apoptosis pathway, including pro-apoptotic factors downstream of the ATF3-CHOP cascade, were dramatically up-regulated. Altogether our findings add new pieces to the understanding of CSB mechanisms of action and to the molecular basis of CS syndrome.

Introduction

Apoptosis evasion is a fundamental hallmark used by cancer cells to evolve resistance to cell death induced in response either to the intrinsic perturbation of metabolic circuitries or to anti-cancer drug therapies [1]. The ability to evade apoptosis is caused by a range of different alterations including the over-expression of anti-apoptotic factors, which bring back to sub-lethal levels the stress conditions associated to cancer cell metabolism [2]. Suppression of these anti-apoptotic factors might re-sensitize cancer cells to apoptosis and offer new therapeutical strategies in alternative or in association with conventional chemotherapy.

CSB is a member of the SWI/SNF ATP-dependent chromatin remodelling protein family that can wrap DNA and remodel chromatin [3–5]. Mutations in the *csb* gene lead to Cockayne syndrome (CS), a rare human autosomal recessive disorder characterized by a progressive degeneration of a wide range of tissues and organs and features of premature aging [6,7]. CSB participates in a number of different functions of a cell metabolism. It plays a role in transcription-coupled repair (TCR), an important sub-pathway of nucleotide excision repair (NER) that rapidly removes bulky DNA lesions located on the transcribed strand of active genes [8]. In addition, CSB plays a role during basal and activated transcription by stimulating all three classes of nuclear RNA polymerases [4,9,10]. Finally, CSB has been demonstrated to be a key regulator of p53, stimulating its ubiquitination and degradation, therefore re-equilibrating the physiological response toward cell proliferation and survival rather than cell cycle arrest and cell death upon stress [11–13]. Along these lines we speculated that CSB functions as an anti-apoptotic factor [14].

In a recent study, we demonstrated that a number of cancer cell lines from different tissues display dramatically increased expression of CSB protein and that its ablation induces massive cell death via apoptosis [15]. Interestingly, normal and cancer cell lines displaying normal expression of CSB remained unaffected when this protein was suppressed. The fact that CSB ablation specifically affects tumor cells, without harming non-transformed cells, suggests that the former are addicted to elevated levels of CSB. Here we investigated the effects on global gene expression in HeLa cells, caused by CSB silencing, in order to elucidate the molecular mechanism by which CSB depletion causes massive apoptosis in cancer cells.

Results

Microarray gene expression profile of Hela cells suppressed for CSB protein

We have recently shown that CSB ablation induces a pro-apoptotic effect [15]. To gain insights into the mechanisms underlying this pro-apoptotic effect we performed genome wide gene expression analysis. For this purpose, cells were incubated with antisense oligonucleotides specifically inducing CSB mRNA degradation (ASO). Moreover, we used three different experimental controls: mock treated cells (CTRL), transfection reagents alone (OLF) and cells treated with sense oligonucleotides (SO). Two biological replicates were performed for each experimental point and two time points (6 and 12 h) were chosen in order to study the early perturbations in the transcriptome arising from the suppression of CSB (Fig 1A). Relative CSB expression was verified by qRT-PCR, for each experimental point, as shown in Fig 1B. A reduction of around 60% (std 0.02) and 80% (std 0.015) in CSB mRNA expression was detected at 6 and 12h, after transfection, respectively. As expected, suppression of CSB results in massive induction of apoptosis (57% of cells + 9.3 std) and a strong reduction of cell viability, at 48h post transfection (Fig 1C).

Global gene expression patterns were then determined using microarrays (Agilent SurePrint G3 Human GE 8x60K) representing the entire transcriptome. Using a multiples response method with a FDR (false discovery rate) < 0.05 we found that there were hundreds of genes differentially regulated across the different conditions (S1 Table).

We analyzed the hierarchical clustering and performed principal component analysis of mRNA expression profiles. Good reproducibility for each experimental point was demonstrated by the hierarchical clustering (Fig 1D). The only exception highlighted concerns a partial mismatch between OLF and CTRL, at 12h. In the principal component analysis, the PC1 axis clearly distinguished the experimental points referred to 6 and 12 hours while the PC2 clearly distinguished between control samples (CTRL, OLF and SO) and CSB suppressed cells

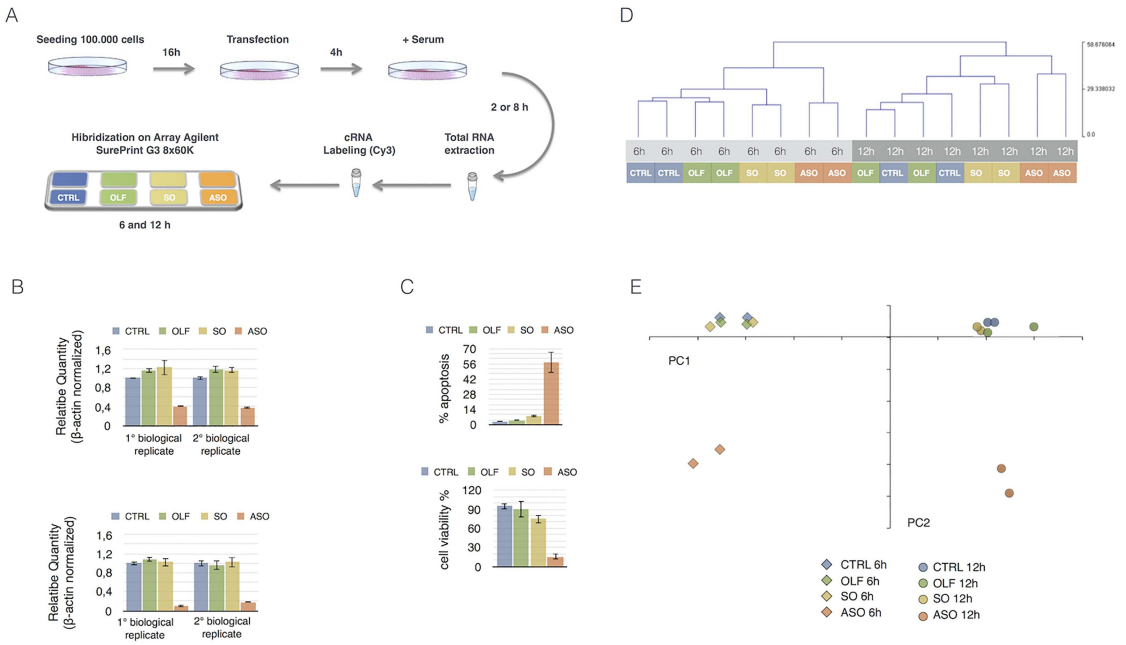

Fig 1. A) Experimental design: briefly cells were seeded at the confluence of $1X10^5$ cells and transiently transfected 16 h later with ASO or SO or simply exposed to the transfectant reagent (OLF). Cells were recovered 2h or 8h (6h and 12h after the start of the transfection) after the adding of the serum. Total RNA was used as starting material to generate labeled cRNA for successive array hybridization. Two biological samples for each experimental point were analyzed. B) Graphs showing qRT-PCR analysis of CSB mRNA expression, at 6h (upper panel) and 12h (lower panel) after the transfection for both the biological replicates. The results, normalized to β-actin, were averaged from values obtained by performing three technical replicates. The values are means ± SD. C) Graphs showing apoptosis and cell viability percentage 48h after CSB ablation. The results were averaged from values obtained by performing three technical replicates. The values are means ± SD. D) Hierarchical clustering of samples, obtained using a selection of all filtered: 17703 probes that have a |Dev.st/Mean = CV|<5% in Log2 expression values between biological replicates, across all samples. E) Principal Component Analysis of samples, using a selection of all filtered: 17703 probes that have a |Dev.st/Mean = CV|<5% in Log2 expression values between biological replicates, across all samples.

doi:10.1371/journal.pone.0172399.g001

(ASO) (Fig 1E). Interestingly the samples derived from CTRL-, OLF- and SO- treated cells clustered together while the ASO dramatically departed.

The gene list was initially filtered with the cut-off criteria FDR≤0.05 and absolute fold change |FC|≥1.5. Gene expression profiling revealed genes regulated uniquely by ASO, SO and OLF as compared to CTRL sample. To identify those genes whose expression level changed significantly and uniquely in response to CSB suppression we used a pair-wise comparison between ASO and CTRL, ASO and OLF, finally ASO and SO. In Fig 2 we represent the overlap between these sets of genes using Venn diagrams. Suppression of CSB affects the expressionof 528 (213 down-regulated and 315 up-regulated) genes at 6h and 558 (444 down-regulatedand 114 up-regulated) genes at 12h.

Functional analysis of differentially expressed genes

To further understand the mechanisms by which CSB ablation induces apoptosis, differentially expressed genes (DEGs) obtained from the primary analysis were annotated by Gene Ontology (GO) to identify the Biological Process affected; enrichment analysis on up- and down-regulated genes was carried out using the DAVID web tool. A P-value < 0.05 and a Fold Enrichment (FE) value > 2 were chosen as cut off criteria. FE was calculated by dividing the frequency of specific gene cluster to the total frequency for each GO term.

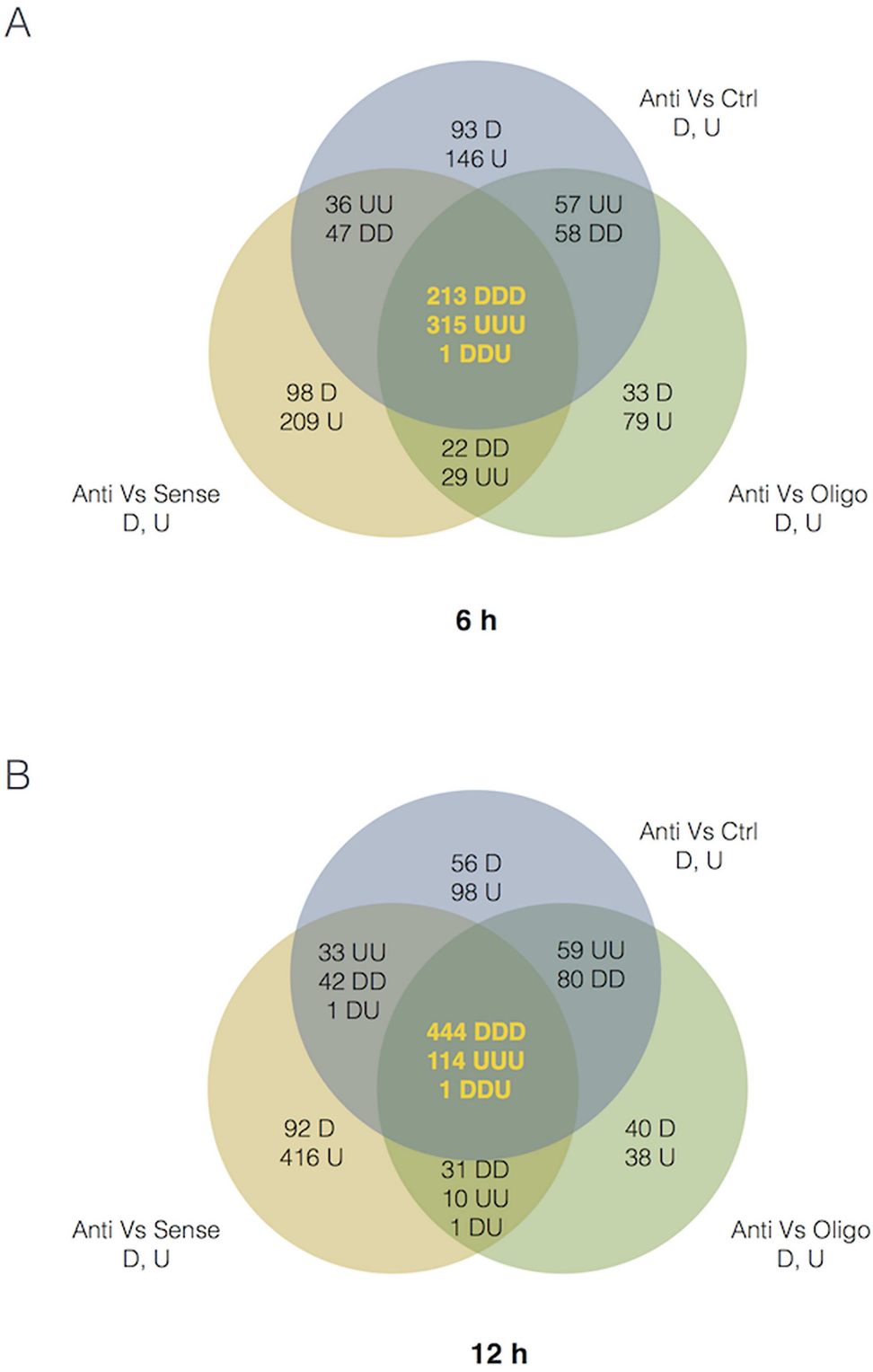

Fig 2. Venn diagrams showing pair-wise comparison between ASO and CTRL, ASO and OLF, finally ASO and SO at 6h and 12h. For intersections letters are in clockwise order of, for example DD for {Anti vs Ctrl} Intersect {Anti vs Oligo} means *first* D in {Anti vs Ctrl} and *second* D in {Anti vs Oligo}. Concerning the central intersection (yellow numbers) the clockwise order starts from Anti vs Ctrl. D means down-regulated and U up-regulated.

doi:10.1371/journal.pone.0172399.g002

Table 1.

6h			
GO ID	**Terms**	**Fold Enrichment**	**P-value**
GO:1990440	Positive regulation of transcription from RNA polymerase II promoter in response to endoplasmic reticulum stress	22.76	2.86E-02
GO:0070059	Intrinsic apoptotic signaling pathway in response to endoplasmic reticulum stress	15.86	7.67E-05
GO:0030968	Endoplasmic reticulum unfolded protein response	5.91	1.17E-02
GO:0034620	Cellular response to unfolded protein	5.75	1.54E-02
GO:0035967	Cellular response to topologically incorrect protein	5.33	3.30E-02
GO:0044843	Cell cycle G1/S phase transition	4.72	2.12E-02
GO:0042594	Response to starvation	4.53	3.42E-02
GO:0072331	Signal transduction by p53 class mediator	4.50	3.65E-02
12h			
GO ID	**Terms**	**Fold Enrichment**	**P-value**
GO:0070059	Intrinsic apoptotic signaling pathway in response to endoplasmic reticulum stress	12.58	2.95E-03
GO:0006986	Response to unfolded protein	5.42	2.73E-04
GO:0030968	Endoplasmic reticulum unfolded protein response	5.27	3.75E-02
GO:0034620	Cellular response to unfolded protein	5.13	4.89E-02
GO:0035966	Response to topologically incorrect protein	5.05	7.24E-04
GO:0034976	Response to endoplasmic reticulum stress	4.60	4.89E-05
GO:0031396	Regulation of protein ubiquitination	3.58	2.21E-02
GO:0008380	RNA splicing	3.16	9.38E-03

GO: Gene Ontology

doi:10.1371/journal.pone.0172399.t001

Table 1 illustrates the FE of the major GO terms at 6h and 12h after the suppression of CSB. Altogether, gene ontology analysis revealed that responses to endoplasmic reticulum stress and to unfolded proteins, and induction of cell apoptosis in response to endoplasmic reticulum stress were ranked in the top cellular events being induced, and that the major components of endoplasmic reticulum stress-mediated apoptosis pathway were over-represented.

With the aim to reduce the number of genes to focus our attention on, we further filtered the list to retain those genes which showed a fold change > 2 (ASO vs SO), and belonged to the top GO terms listed above. The list of genes so obtained is showed in Figs 3 and 4, for 6h and 12h, respectively. Activating transcription factor 3 (ATF3), a member of the ATF/cAMP response element binding protein (CREB) family of transcription factors induced by several stressors including ER stress, displays a dramatic increase (9.58 folds ASO vs SO) at 6h. Microarray data showed a 3.9 and 2 fold increase (ASO vs SO), at 6 and 12 h respectively, in CHOP, known to be the main mediator of ER stress-induced apoptosis. Along this line, CHAC1, PPP1R15A, BBC3 (PUMA), TRIB3 and NUPR1, pro-apoptotic components of unfolded protein response downstream of ATF3-CHOP cascade, showed a fold increase of 5.31, 3.9, 3.1, 2.97 and 2.16 respectively, at 6h. Moreover, with the exception of BBC3, the up-regulation of those genes is maintained also at 12h. In addition, general mediators of apoptosis and cell cycle arrest, such as INHBA, GADD45a and ASNS were also among the genes up-regulated in response to CSB suppression both at 6 and 12h.

Microarray data revealed a reduction in the gene expression of molecular chaperons and co-chaperons, including heat shock proteins (TCP1, HSPA4, HSPA1A, HSPD1, SACS, ST13, DNAJC21, STIP1, PSMC6, ST13) in either or both the times points. In addition, PSMD6,

PSMD5, PSMB5, PSMC4 and PSMC6 subunits of the protease/chaperone complex proteasome 26S were also down regulated as were a number of splicing factors (RBM35, CWC22, C1QBP, RALY).

Validation of microarray analysis data by quantitative real-time PCR

As validation step of the microarray analysis results, relative expression of genes reported in Figs 3 and 4 was also measured by qRT-PCR using specific primer sets. Expression levels of each gene, either at 6 or 12 h, in OLF, SO and ASO treated cells have been compared to CTRL (Fig 5). As indicated by the graphs, for most of genes analysed, all the three controls samples (CTRL, OLF and SO) behave similarly while the CSB suppressed sample strongly diverges. To evaluate the correlation between microarray and qRT-PCR data, we calculated the $\log_2$ of fold changes of all selected genes in the CSB suppressed cells (ASO) relative to the control (CTRL) obtained from both the platform and tested the correlation between these two sets of data. Our results indicated a robust consistency between microarray and qRT-PCR data either at 6 and 12 h ($R^2 = 0.84$, $P < 0.0001$ at 6h; $R^2 = 0.63$, $P < 0.0001$ at 12h; Fig 6).

Next, to validate the above results, we analyzed by Western blotting the expression of proteins playing a key role in UPR. As showed in Fig 7A, the phosphorylation of eIF2α, which is triggered by the activation of ER resident transmembrane protein kinase PERK, one of the major sensor proteins which can detect the protein-folding imbalance generated by ER stress, is induced in CSB suppressed cells (ASO) compared to three different experimental controls. Accordingly, we observed that suppression of CSB also gave rise to an increased expression of ATF4, a master regulator of the UPR response and the pro-apoptotic transcription factor CHOP, both downstream targets of eIF2α phosphorylation.

Finally, with the aim to understand if suppression of CSB would cause ER stress also in other cell lines, we knocked down CSB in the neuroblastoma cells SKNBE-2c. ASO-induced suppression of CSB (Fig 7B) determined a strong induction of apoptosis (Fig 7C) and a correlated decrease of cell viability (Fig 7D). As illustrated in Fig 7E, RT-PCR revealed that suppression of CSB enhanced the expression of genes involved in the UPR response, as illustrated by the increased expression of ATF3, CHOP, CHAC1, NUPR1 and NOXA. Therefore the effect of CSB suppression on UPR response are not cell type specific.

Discussion

Our findings reveal that HeLa cells are addicted to the elevated levels of CSB protein expression and that response to unfolded proteins and to endoplasmic reticulum stress is triggered upon CSB suppression. Furthermore, major components of UPR-mediated apoptosis pathway, including pro-apoptotic factors downstream of the ATF3-CHOP cascade, such as CHAC1, TRIB3, GADD34 and ASNS, are dramatically up-regulated and at the origin of the massive induction of apoptosis, displayed by HeLa cells upon CSB suppression. A similar behavior was also displayed when CSB was suppressed in neuroblastoma cells. One interesting question is why the outcome of the UPR response is only the activation of proapoptotic genes. Indeed UPR response also involves transcriptional induction of ER chaperone genes to enhance folding capacity and transcriptional induction of ER-associated degradation (ERAD) genes to increase protein degradation capacity [16–18]. All this responses are needed in order to maintain a productive ER protein folding environment and promote cell survival. It is only when these adaptive mechanisms fail to resolve protein folding defect that the UPR response tips the balance towards apoptosis by up regulating the ATF3-CHOP cascade [19–21].

In contrast, we observed that all these adaptive (pro-survival) mechanisms are down-regulated, upon CSB suppression. Chaperons folding protein-coding genes, such as TCP1,

Protein	Antisense vs Sense		Antisense vs CTRL		Sense vs CTRL		Functions
	Fold change	Test.t	Fold change	Test.t	Fold change	Test.t	
ATF3	9,58	9,35E-04	15	6,21E-04	1,53	2,49E-02	Member of the ATF/CREB subfamily of basic-region leucine zipper (bZIP) proteins, is induced in response to endoplasmic reticulum (ER) stress.
CHAC1	5,31	5,49E-03	6,77	9,9E-04	1,27	2,55E-02	Acts as a pro-apoptotic component of the unfolded protein response pathway by mediating the pro-apoptotic effects of the ATF4-ATF3-CHOP cascade
INHBA	5,06	5,74E-03	4,20	3,24E-02	0,83	2,43E-01	Inhibin has been shown to regulate gonadal stromal cell proliferation negatively and to have tumor-suppressor activity
CHOP	3,88	8,34E-04	5,06	8,001E-04	1,18	1,49E-02	Multifunctional transcription factor in ER stress response. Induces cell cycle arrest and apoptosis in response to ER stress.
PPP1R15A	3,9	3,27E-05	4,63	1,27E-02	1,18	1,13E-01	Stress induced gene. Plays a role in the recovery of the translation during ER stress. Is involved in apoptosis.
SESN2	3,36	3,27E-05	3,73	2,96E-02	1,11	2,76E-01	The encoded protein may function in the regulation of cell growth and survival. Is involved in ER stress and the induction of the autophagy
BBC3 (PUMA)	3,10	4,6E-03	3,78	4,74E-02	1,22	2,52E-01	This gene encodes a member of the BCL-2 family of protein. Cooperates with direct activator proteins to induce mitochondrial apoptosis
FOSB	3,05	1,37E-02	4,47	2,95E-02	1,46	9,73E-02	This gene encodes a leucine zipper protein implicated in the induction of apoptosis in cells in response to stress factors and growth factor withdrawal
TRIB3	2,97	8,15E-04	3,86	6,67E-04	1,30	6,91E-03	This protein is induced during ER stress by ATF4-CHOP pathway. It is involved in cell death
GDF15	2,75	1,55E-03	2,87	8,53E-03	1,04	2,43E-01	The protein encoded by this gene belongs to the transforming growth factor-beta (TGF-beta) family. Inducer of apoptosis.
JUN	2,73	1,92E-03	2,73	1,92E-03	1,28	1,39E-01	Transcription factor. Up-regolation of this protein inhibits proliferation and induces apoptosis
KLF6	2,62	6,03E-03	2,71	4,74E-03	1,06	3,2E-01	KLF6 suppresses tumor growth and induces apoptosis in cancer cells through ATF3 expression
KLF4	2,62	1,19E-02	2,77	3,14E-03	1,06	2,05E-01	Zinc-finger transcription factor. Overexpression of this protein is associated with cell proliferation and cell cycle arrest and with induction of apoptosis .
GADD45A	2,58	1,89E-03	2,95	1,78E-02	1,14	1,98E-01	This gene is induced by DNA damaging agents and other cellular stresses. It is induced by ATF4, mediates apoptosis ER stress-induced.
ASNS	2,39	5,54E-03	1,56	4,06E-02	0,54	4,74E-02	Pro-apoptotic gene induced by ATF4 during ER stress
JUND	2,22	1,67E-02	2,79	1,77E-02	1,23	6,8E-02	Transcription factor involved in induction of apoptosis during stress condition
NUPR1	2,16	5,11E-02	2,17	5,69E-02	1,00	4,86E-01	Involved in apoptosis via upregulation of the ER stress-related genes, ATF4, CHOP, and TRIB3
AEN	2,13	8,09E-03	2,13	5,93E-03	1,00	4,95E-01	Exonuclease with activity against single- and double- stranded DNA and RNA. Mediates p53-induces apoptosis
KLF10	2,13	6,92E-03	2,23	2,56E-02	1,05	2,96E-01	Involved in inhibition of cell proliferation and induction of apoptosis
IER3	2,08	2,69E-02	2,46	2,03E-02	1,18	1,54E-01	Glycoprotein that regulates death receptor–induced apoptosis, interacts with NF-KB pathways, and increases expression rapidly in response to cellular stresses .
PMAIP1 (NOXA)	2,08	6,39E-04	2,22	8,78E-04	1,06	5,92E-02	Promotes activation of caspase and apoptosis. Promotes mitochondrial membrane changes and efflux of apoptogenic proteins from the mitochondria
BTG1	2,04	1,84E-03	2,03	3,84E-02	0,99	4,89E-01	This gene is a member of an anti-proliferative gene family that regulates cell growth and differentiation
RBM25	4,55	8,83E-03	4,89	7,54E-03	1,06	1,08E-01	RNA-binding protein that acts as a regulator of alternative pre-mRNA splicing. Involved in apoptotic cell death.
C1QBP	4,35	3,41E-02	4,89	3,07E-02	1,14	1,69E-02	Is believed to be a multifunctional protein involved in inflammation and infection processes, ribosome biogenesis and regulation of apoptosis.
TCP1	4,00	1,10E-02	4,32	9,98E-03	1,09	2,58E-01	The protein encoded by this gene is a molecular chaperone that is a member of the chaperonin containing TCP1 complex (CCT).
ERGIC2	3,33	2,48E-02	3,46	1,17E-02	1,02	3,92E-01	Protein that may have a role in transport between ER and Golgi .
ST13	3,13	2,44E-02	3,23	2,50E-02	1,02	2,82E-01	The protein encoded by this gene is an adaptor protein that mediates the association of the heat shock proteins HSP70 and HSP90
RPS17	2,86	3,36E-02	2,71	1,50E-02	0,95	2,97E-01	This gene encodes a ribosomal protein that is a component of the 40S subunit
CWC22	2,70	5,43E-03	2,41	1,69E-02	0,89	2,52E-01	Required for pre-mRNA splicing and for exon-junction complex (EJC) assembly
PSMD6	2,38	1,93E-02	2,62	2,01E-02	1,11	9,21E-02	This protein is a subunit of the 26S proteasome which colocalizes with DNA damage foci and is involved in the ATP-dependent degradation of ubiquinated protein
KIF1C	2,27	6,85E-04	2,30	2,58E-02	1,01	4,77E-01	Motor required for the retrograde transport of Golgi vesicles to the endoplasmic reticulum
RAB13	2,27	5,43E-03	2,60	1,69E-02	1,16	7,84E-02	This gene is a member of the Rab family of small G proteins and plays a role in regulating membrane trafficking between trans-Golgi network and endosomes (RE)
HSPA4	2,22	5,50E-02	2,01	5,97E-02	0,90	6,39E-02	Belongs to the heat shock protein 70 family. ER stress related protein.
TRAPPC3	2,13	6,62E-03	2,31	9,89E-05	1,08	9,53E-02	This protein may play a role in vesicular transport from endoplasmic reticulum to Golgi
HSPA1A	2,13	3,05E-03	2,14	7,85E-03	1,01	4,58E-01	Belongs to the heat shock protein 70 family. In conjuction with other heat shock proteins.
SELK	2,08	5,01E-02	1,73	6,59E-02	0,84	6,76E-03	This is a selenoprotein increased under ER stress condition that plays a key role during endoplasmic reticulum-associated degradation (ERAD)
DDX39B	2,04	4,67E-02	2,07	2,88E-02	1,02	4,49E-01	This protein is involved in nuclear export of spliced and unspliced mRNA.
HSPD1	2,04	3,05E-02	1,59	7,71E-02	0,78	1,64E-01	This gene encodes a member of the chaperonin family. May facilitate the correct folding of imported proteins. Plays a role during ER stress
SACS	2,00	2,64E-02	1,84	1,34E-02	1,00	2,07E-01	Co-chaperone which acts as a regulator of the Hsp70 chaperone machinery
STX8	1,96	1,45E-02	2,20	1,93E-03	1,10	7,17E-02	Vesicle trafficking protein that functions in the early secretory pathway, possibly by mediating retrograde transport from cis-Golgi membranes to the ER

Fig 3. Filtered list of genes which showed a fold change > 2 (ASO vs SO) in the microarray analysis at 6h, and belonged to the top GO terms listed in Table 1.

doi:10.1371/journal.pone.0172399.g003

Protein	Antisense vs Sense		Antisense vs CTRL		Sense vs CTRL		Functions
	Fold change	Test.t	Fold change	Test.t	Fold change	Test.t	
CHAC1	3,81	1,13E-02	5,38	1,35E-02	1,41	7,51E-02	Acts as a pro-apoptotic component of the unfolded protein response pathway by mediating the pro-apoptotic effects of the ATF4-ATF3-CHOP cascade
ASNS	3,23	8,61E-03	2,38	2,77E-02	1,36	4,90E-02	Pro-apoptotic gene induced by ATF4 during ER stress
TRIB3	2,77	1,89E-02	3,25	2,09E-02	1,17	2,20E-01	This protein is induced during ER stress by ATF4-CHOP pathway. It is involved in cell death
INHBA	2,75	2,63E-02	2,95	2,52E-02	1,07	3,96E-01	Inhibin has been shown to regulate gonadal stromal cell proliferation negatively and to have tumor-suppressor activity
NUPR1	2,64	6,61E-03	3,01	5,18E-03	1,14	1,66E-01	Involved in apoptosis via upregulation of the ER stress-related genes, ATF4, CHOP, and TRIB3
FAM129A	2,50	6,76E-02	2,93	3,21E-02	1,17	2,96E-01	Regulates phosphorylation of a number of proteins involved in translation regulation including EIF2A, EIF4EBP1 and RPS6KB1. May be involved in the endoplasmic reticulum stress response
SESN2	2,48	5,71E-02	4,08	1,78E-03	1,65	9,88E-02	The encoded protein may function in the regulation of cell growth and survival. Is involved in ER stress and the induction of the autophagy
DCLK1	2,46	1,81E-02	1,99	1,47E-02	0,81	3,86E-02	The encoded protein is involved in several different cellular processes, including neuronal migration, retrograde transport, neuronal apoptosis and neurogenesis
JUN	2,22	3,56E-02	2,73	9,37E-03	1,23	2,04E-01	Transcription factor. Up-regolation of this protein inhibits proliferation and induces apoptosis
PPP1R15A	2,10	2,80E-02	3,73	3,20E-02	1,78	5,82E-02	Stress induced gene. Plays a role in the recovery of the translation during ER stress. Is involved in apoptosis.
BEX2	2,08	7,33E-02	2,30	4,23E-02	1,10	2,9E-01	Regulator of mitochondrial apoptosis and G1 cell cycle in breast cancer
CHOP	2,04	2,52E-02	3,36	2,08E-02	1,30	2,00E-02	Multifunctional transcription factor in ER stress response. Induces cell cycle arrest and apoptosis in response to ER stress.
C1QBP	9,09	2,67E-02	12,50	2,71E-02	1,22	4,68E-02	Is believed to be a multifunctional protein involved in inflammation and infection processes, ribosome biogenesis and regulation of apoptosis.
RBM25	7,69	5,32E-03	9,09	1,88E-03	1,03	3,97E-01	RNA-binding protein that acts as a regulator of alternative pre-mRNA splicing. Involved in apoptotic cell death.
PSMC6	6,77	3,72E-02	6,77	3,57E-02	1,00	4,81E-01	This gene encodes one of the ATPase subunits of 26S proteasome which have a chaperone-like activity.
ERGIC2	4,55	1,64E-03	4,76	7,04E-03	1,11	1,66E-01	Protein that may have a role in transport between ER and Golgi .
CSNK2A2	4,47	1,46E-02	3,89	1,89E-02	0,87	3,25E-02	Serine/threonine protein kinase that is thought to have a regulatory function in cell proliferation, cell differentiation and apoptosis
GPS1	4,23	9,07E-03	3,51	1,66E-02	0,83	2,02E-01	Essential component of the COP9 signalosome complex (CSN), a complex involved in various cellular and developmental processe
ETF1	3,56	4,11E-03	3,73	1,58E-02	1,05	3,25E-01	The encoded protein plays an essential role in directing termination of mRNA translation
SACS	3,33	1,27E-03	3,45	1,07E-03	1,00	4,97E-01	Co-chaperone which acts as a regulator of the Hsp70 chaperone machinery
SELK	3,23	1,88E-02	3,03	2,93E-02	0,93	2,08E-01	This is a selenoprotein increased under ER stress condition that plays a key role during endoplasmic reticulum-associated degradation (ERAD)
PSMD6	3,23	3,50E-02	3,23	3,59E-02	1,00	4,71E-01	This protein is a subunit of the 26S proteasome which colocalizes with DNA damage foci and is involved in the ATP-dependent degradation of ubiquinated protein
PSMC4	3,18	1,99E-02	3,10	3,75E-02	0,97	4,21E-01	This gene encodes a member of the triple-A family of ATPases that is a component of the 19S regulatory subunit and plays a role in 26S proteasome assembly
ST13	3,13	1,12E-02	3,23	1,27E-02	1,03	4,05E-01	The protein encoded by this gene is an adaptor protein that mediates the association of the heat shock proteins HSP70 and HSP90
TRAPPC3	3,03	5,45E-02	3,33	4,24E-02	1,06	2,42E-01	This protein may play a role in vesicular transport from endoplasmic reticulum to Golgi
TCP1	2,94	1,22E-02	2,78	3,28E-02	0,93	2,21E-01	The protein encoded by this gene is a molecular chaperone that is a member of the chaperonin containing TCP1 complex (CCT).
RAB13	2,94	5,59E-03	3,45	1,43E-02	1,15	2,11E-01	This gene is a member of the Rab family of small G proteins and plays a role in regulating membrane trafficking between trans-Golgi network and endosomes (RE)
HSPA4	2,86	2,34E-03	2,86	1,01E-02	0,99	3,98E-01	Belongs to the heat shock protein 70 family. ER stress related protein.
HSPB1	2,85	5,26E-02	2,62	5,64E-03	0,92	3,6E-01	Heat shock protein involved in stress resistance and actin organization
CWC22	2,78	6,00E-02	2,94	7,07E-03	1,04	4,33E-01	Required for pre-mRNA splicing and for exon-junction complex (EJC) assembly
DDX39B	2,70	3,49E-03	2,94	4,20E-03	1,09	1,7E-01	This protein is involved in nuclear export of spliced and unspliced mRNA.
PSMB5	2,68	6,45E-02	2,62	5,62E-02	0,98	4,16E-01	This protein is a subunit of 26S proteasome
RPS17	2,63	3,24E-02	2,56	5,71E-02	0,97	4,52E-01	This gene encodes a ribosomal protein that is a component of the 40S subunit
EDC4	2,57	3,52E-02	2,51	1,39E-02	0,98	3,99E-01	In the process of mRNA degradation, seems to play a role in mRNA decapping
PSMD5	2,41	5,76E-02	2,75	2,19E-02	1,14	2,6E-01	Acts as a chaperone during the assembly of the 26S proteasome.
SEPT2	2,28	1,69E-02	2,83	1,30E-02	1,24	3,94E-02	Filament-forming cytoskeletal GTPase required for normal organization of the actin cytoskeleton
RALY	2,25	2,95E-02	2,03	4,96E-02	0,90	3,14E-01	The protein may be involved in pre-mRNA splicing
EIF2B4	2,25	5,11E-02	2,14	6,80E-02	0,95	3,96E-01	The eukaryotic initiation factor 2B is necessary for protein synthesis
STX8	2,22	4,19E-03	2,70	4,73E-03	1,20	3,52E-02	Vesicle trafficking protein that functions in the early secretory pathway, possibly by mediating retrograde transport from cis-Golgi membranes to the ER
WRNIP1	2,16	1,03E-02	1,87	4,27E-02	0,86	1,92E-01	This protein functions as a modulator for initiation or reinitiation events during DNA polymerase delta-mediated DNA synthesis.
NF1	2,16	4,54E-02	2,10	4,37E-02	0,97	3,87E-01	This protein appears to function as a negative regulator of the RAS signal transduction pathway
STIP1	2,11	4E-02	2,19	5,70E-02	1,04	4,33E-01	This protein is an adaptor protein that coordinates the functions of HSP70 and HSP90 in protein folding
RABL2A	2,08	1,05E-03	2,38	1,60E-03	1,14	4,89E-02	The proteins in the family of RAS-related signaling molecules are small GTP-binding proteins that play important roles in the regulation of exocytotic and endocytotic pathways
DOLK	2,04	2,58E-02	1,85	5,28E-02	0,91	1,61E-01	This protein is essential for biosynthesis of glycosyl phosphatidylinositol anchors in endoplasmic reticulum.
ABCB10	2,04	2,89E-02	2,03	3,30E-02	1,00	4,91E-02	The membrane-associated protein encoded by this gene is a member of the superfamily of ATP-binding cassette (ABC) transporters. ABC proteins transport various molecules across extra- and intra-cellular membranes.
DNAJC21	2,00	7,49E-03	1,75	3,41E-02	0,86	1,92E-01	May act as a co-chaperone for HSP70
RANBP9	2,00	4,11E-02	2,28	1,66E-02	1,09	2,92E-01	This gene encodes a protein that binds RAN, a small GTP binding protein belonging to the RAS superfamily that is essential for the translocation of RNA and proteins through the nuclear pore complex

Fig 4. Filtered list of genes which showed a fold change > 2 (ASO vs SO) in the microarray analysis at 12h, and belonged to the top GO terms listed in Table 1.

doi:10.1371/journal.pone.0172399.g004

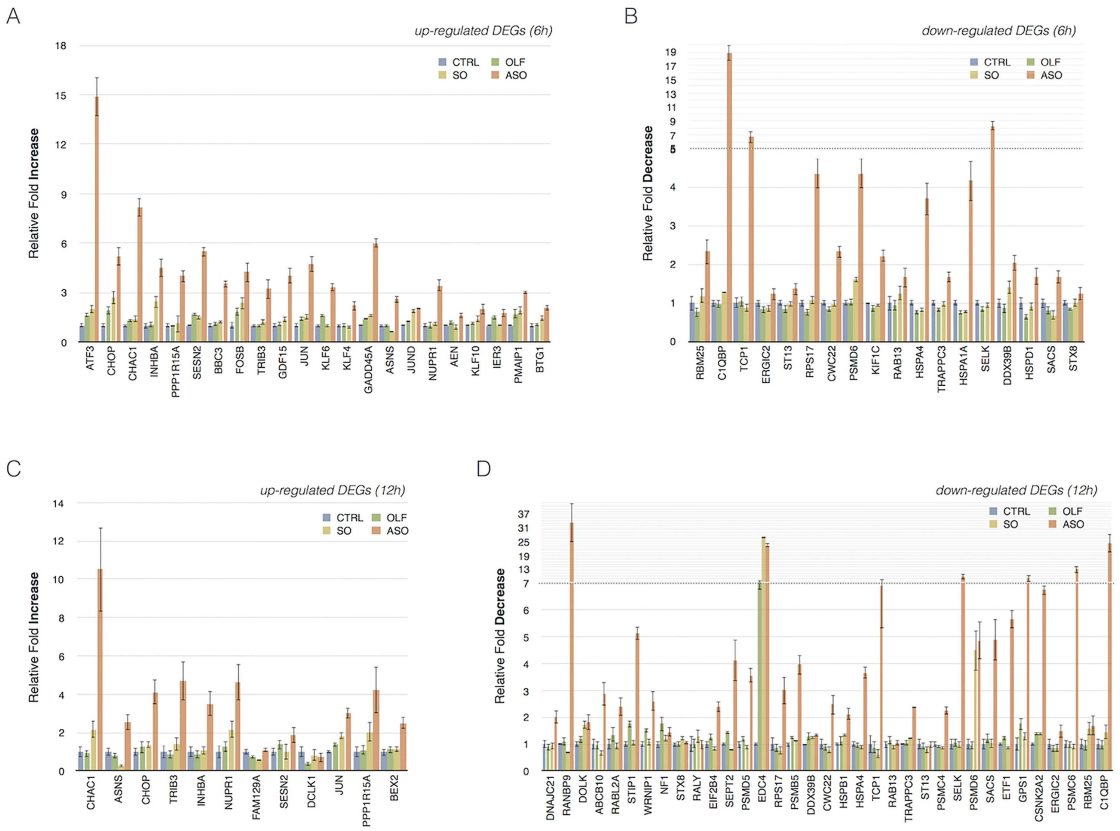

Fig 5. qPCR verification of DEGs. Graphs show relative fold change values of up-regulation (A and C) and down regulation (B and D) of selected genes. The results, normalized to β-actin, were averaged from values obtained by performing three technical replicates. The values are means ± SD.

doi:10.1371/journal.pone.0172399.g005

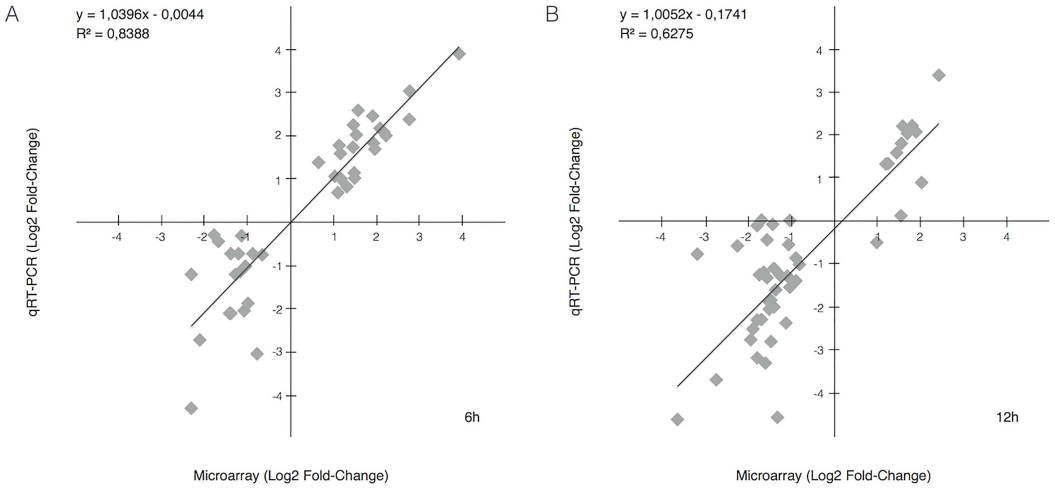

Fig 6. Validation of microarray data with qRT-PCR. Correlation between qRT-PCR and microarray analysis at 6h (A) and 12h (B). The correlation coefficients (R^2) are 0.83 and 0.62, respectively.

doi:10.1371/journal.pone.0172399.g006

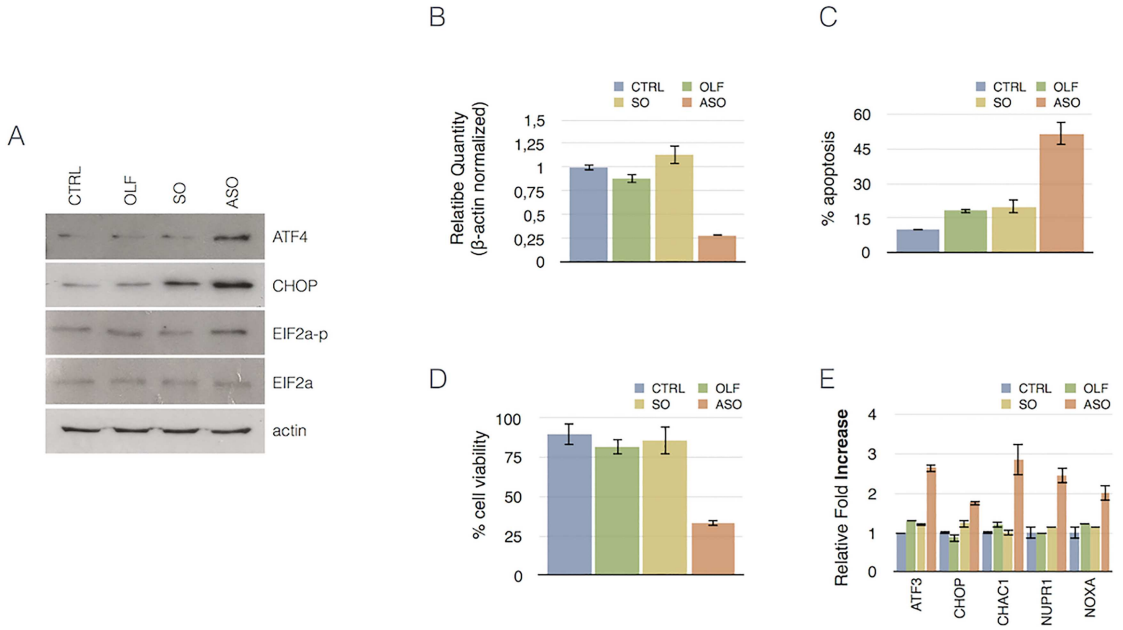

Fig 7. Western blotting demonstrating the significant increase of ATF4, CHOP and EIF2a-p after CSB knockdown. B) Graphs showing qRT-PCR analysis of CSB mRNA expression in SKNBE-2c cells, at 12h after the transfection. The results, normalized to β-actin, were averaged from values obtained by performing three technical replicates. The values are means ± SD. Graphs showing apoptosis (C) and cell viability (D) percentage in SKNBE-2c cells 48h after CSB ablation. The results were averaged from values obtained by performing three technical replicates. The values are means ± SD. E) Graphs show relative fold change values of up-regulation of selected genes in SKNBE-2c cells. The results, normalized to β-actin, were averaged from values obtained by performing three technical replicates. The values are means ± SD.

doi:10.1371/journal.pone.0172399.g007

HSPA1A, HSPA4 and HSPD1, are down-regulated as well. Along the same line, expression of SELK, involved in ERAD, is also down-regulated. Down-regulation of mediators of UPR pro-survival pathway and up-regulation of mediators of UPR pro-death pathway upon CSB suppression might be explained in the context of transformed cells (HeLa and SKNBE-2c). Activation of pro-survival UPR response is an adaptive survival strategy that cancer cells adopt to deal with the increasing levels of ER stress determined by their increased anabolism (increased protein production, mTOR activation) and hostile environmental (hypoxia, nutrient deprivation, reactive oxygen species (ROS) and redox changes) [22]. Activation of pro-apoptotic genes upon CSB suppression conjointly with down-regulation of adaptive pro-survival genes let us speculate that ablation of CSB determines, in cancer cells, an increase of the (pre-existing) ER stress that tip the balance from pro-survival towards apoptosis signalling.

This opens a new scenario for the role played by CSB in tumour biology. What is CSB role in limiting ER stress? Is CSB involved in protein folding? These are new and exciting areas that warrant investigation.

Hallmarks of cancer are prone to induce stress at various levels. Oxidative stress, hypoxia and ER stress are something that the cancer are to deal with [23–27]. Furthermore, all these processes are interdependent. Therefore, cancer cells have to cope with multiple stress conditions at once, all prone to induce apoptosis.

It is known that CSB protein counteracts oxidative stress detrimental effect. Some authors have recently shown that CSB-mutated cells have increased levels of intra-mitochondrial ROS suggesting that CSB might behave as an electron scavenger in the mitochondria and that its absence leads to increased oxidative damage [28]. We showed that CSB also favours pro-

survival HIF-1 induced response to attenuate the detrimental effect of hypoxia condition [12], including increased generation of mitochondrial ROS [29].

Both oxidative stress and hypoxia, if not adequately contrasted, are known to induce ER stress. ROS can oxidize cysteine residues, leading to excessive disulphide bond formation in proteins and consequent folding alteration [30]. Hypoxia leads to a deficit in the production of ATP and consequently a reduced chaperon activity in the ER that results in impaired protein folding and ER stress [31]. Lastly, it is emerging that CSB together with CSA is associated to the ubiquitin/proteasome system [32–33]. It might be that a reduced presence of CSB could somehow affect the efficiency of protein degradation.

We can speculate that over expression of CSB, as observed in tumours [15], is an adaptive mechanism that the cancer cell develops to counteract hypoxia condition, ROS overproduction and to limit the presence of incorrectly folded proteins, to reduce ER stress.

It has been described that oncogene and tumour suppressor gene mutations might inhibit ER-stress induced apoptosis machinery [27]. Our work, instead, confirms that UPR activation induced cell death is intact in at least some tumour cells and that ER stress and UPR activation may offer a target for combination therapy.

Finally, as well known, CSB mutations result in Cockayne syndrome, a premature aging syndrome characterized by a severe neurodegenerative clinical picture. The importance of the UPR in the process is observed in a number of neurodegenerative diseases including amyotrophic lateral sclerosis, Parkinson's disease, Huntington's disease, Alzheimer's disease and demyelinating neurodegenerative autoimmune diseases such as multiple sclerosis [34–35], which introduces challenges to study the functional significance of ER stress in the pathogenesis of Cockayne syndrome.

Material and methods

Cell culture and gene expression silencing

Cell lines were grown in DMEM (Hela) or a mixture of Eagle's-MEM/F12 (SKNBE-2c) containing 10% FCS and Gentamicin in a 5% CO_2 humidified atmosphere at 37˚C.

For transfection procedure Thermo Fisher Scientific Protocol for Oligofectamine reagent was used. Briefly the day before transfection $1x10^5$ cells were plated in 6-well dishes using medium without antibiotics. Immediately before transfection the medium was replaced with Optimem and oligonucleotides (200 nM final concentration) were delivered using Oligofectamine transfection reagent. The cells were transfected with ASO or SO or simply exposed to the transfectant reagent (OLF). Four hours after transfection Optimem was replaced with fresh complete medium. Total RNA was extracted at 2h or 8h after medium adding. Sense oligonucleotides were the reverse of the antisense sequence. Oligonucleotide sequences are available on request.

Cell viability assay

Cell viability was evaluated using MTT [3-(4,5-dimethylthiazol-2-yl)-2,5-diphenyl-2H-tetrazolium bromide] cell proliferation assay. Cells were plated in 96-well plates one day before oligonucleotides transfection. MTT was added to each well (0.5 mg/ml) 48h after transfection. After incubation for 3 h at 37˚C, the supernatant was replaced with 150ul of solution (10% SDS, 0.6% acetic acid in DMSO) to dissolve the formazan crystals and produce a purple solution. Optical density measurements were obtained using a scanning spectrophotometer DTX 880 Multimode Detector (Beckman Coulter). The readings were made using a 630 nm (background) and a 570 nm filter. The assays were conducted in triplicate for each condition.

Apoptosis analysis

Cells were plated in 6-well plates one day before oligonucleotides transfection as described above; 48 h later the oligonucleotides transfection, a combination of Fluorescein Diacetate (FDA; 15 g/ml), Propidium Iodide (PI; 5 g/ml) and Hoechst (HO; 2 g/ml) were used to differentiate apoptotic and necrotic cells from viable cells. FDA and HO are vital dyes that stain the cytoplasm and nucleus of the viable cells, respectively. The necrotic and the late stage of apoptotic cells are readily identified by PI staining. Cells in the early phase (viable––HO stained) and late phase (dead––PI stained) of apoptosis displayed the characteristic pattern of chromatin fragmentation. Approximately 2000 randomly chosen cells were microscopically analyzed to determine apoptosis levels.

RNA isolation, amplification, labelling and hybridization of microarrays

Total RNA was isolated from HeLa cells using Absolutely RNA Miniprep kit (Agilent Technologies). Quality and Integrity of each sample was checked using Agilent BioAnalyzer 2100 (Agilent RNA 6000 nano kit): samples with a RNA Integrity Number (RIN) index lower than 8.0 were discarded. Aliquots from the same RNA sample, prepared (and pooled) from 3 different experiments were used for the hybridizations to reduce the experimental variability.

All the experimental steps for gene expression profiling, involving the labelling, hybridization and washings of the samples, were done following the one color microarray Agilent protocol (Agilent Technologies, Inc, Santa Clara, CA, USA). CTRL, OLF, SO and ASO samples were labelled with Cy3 and hybridized on Agilent SurePrint G3 Human GE 8x60K Microarrays (grid ID 034494).

Scanning, feature extraction and analysis

Post-hybridization image acquisition was accomplished using the Agilent scanner G2564B, equipped with lasers at 532 nm. Data extraction from the Agilent scanner images was accomplished by Feature Extraction software. Data filtering and analysis were performed using R-Bioconductor and Microsoft Excel. All the features with the flag gIsWellAboveBG = 0 in raw data files (too close to background) were filtered out and excluded from the following analysis. Filtered data were normalized to the 75th percentile.

Data were further filtered by excluding mRNA probes with a coefficient of variation |Dev. st/Mean|>5% in Log2 expression values between biological replicates, across all samples, to obtain a final selection 17703 transcripts.

Differentially expressed genes were selected by a combination of fold change and moderated T-test thresholds by the R-Bioconductor tool Limma (p-value<0.05; |Log2 fold-change ratio| >0.56 equivalent to 1.5 fold in linear scale).

Hierarchical Clustering (HCL) and Principal Component Analysis (PCA) were used to show overall differences between ASO and control samples in transcriptional profiles (Fig 1D and 1E). The analysis of over- and under- represented functional in gene lists annotations was performed using the chart and cluster algorithms of DAVID web tool [36]. The whole microarray dataset is public and available from the Gene Expression Omnibus database (https://www.ncbi.nlm.nih.gov/geo).

Retrotranscription and real-time quantitative PCR

Real-time quantitative PCR was used to verify CSB silencing and the accuracy of microarray data. Total RNA was reverse transcribed for single-stranded cDNA using oligo-$(dT)_{18}$ primer of First Strand cDNA Synthesis kit (Fermentas). Real-time quantitative PCR was carried out

with SYBR green master mixture (Promega) using Mx3005P Real-Time PCR system (Agilent). For quantification of gene expression changes, the Ct method was used to calculate relative fold changes normalized against the housekeeping gene beta actin. To obtain more reliable results, all reactions were performed in triplicate. Primers sequences are available on request.

Concerning microarray data validation, the choice of the mRNA species analyzed by qRT-PCR was made according to the criteria listed in Result.

Supporting information

S1 Table. Differentially expressed mRNA transcripts. The 6 lists correspond to the same 6 comparisons shown in the Venn diagrams of Fig 2. Transcripts were selected, on filtered data-set (see Methods) by a combination of fold change and moderated T-test thresholds by the R-Bioconductor tool Limma (p-value<0.05; |Log2 fold-change ratio| >0.56 equivalent to 1.5 fold in linear scale).
(XLSX)

Acknowledgments

This work was supported by grants from AIRC (IG13074), Telethon (GGP11176), FP7 European Collaborative Project PAINCAGE (603191) and Italian Research Council (EBRI-CNR 2015–2017).

Author Contributions

Conceptualization: LPDS.

Data curation: MC AB RB S. Bongiorni.

Formal analysis: LPDS IA MD.

Funding acquisition: LPDS.

Investigation: MC AB IA MD RB S. Bongiorni S. Brancorsini MF LPDS.

Methodology: LPDS MC MD IA.

Project administration: LPDS.

Resources: LPDS MD.

Software: IA.

Supervision: LPDS MD.

Validation: LPDS MC AB RB IA.

Visualization: LPDS S. Bongiorni MF.

Writing – original draft: LPDS MC AB.

Writing – review & editing: LPDS MC MF.

References

1. Chao MP, Majeti R, Weismann IL (2012) Programmed cell removal: a new obstacle in the road to developing cancer. Nat Rev Cancer 12: 8–67.
2. Portt L, Norman G, Clapp C, Greenwood M, Greenwood MT (2011) Anti-apoptosis and cell survival: a review. Biochim Biophys Acta 1813: 238–59. doi: 10.1016/j.bbamcr.2010.10.010 PMID: 20969895

3. Matson SW, Bean DW, George JW (1994) DNA helicases: enzymes with essential roles in all aspects of DNA metabolism. Bioessays 16: 13–22. doi: 10.1002/bies.950160103 PMID: 8141804
4. Selby CP, Sancar A (1997) Cockayne syndrome group B protein enhances elongation by RNA polymerase II. Proc Natl Acad Sci USA 94: 11205–11209. PMID: 9326587
5. Citterio E, Van Den Boom V, Schnitzler G, Kanaar R, Bonte E, Kingston RE, et al. (2000) ATP-dependent chromatin remodeling by the Cockayne syndrome B DNA repair-transcription-coupling factor. Mol Cell Biol 20: 7643–7653. PMID: 11003660
6. Weidenheim KM, Dickson DW, Rapin I (2009) Neuropathology of Cockayne syndrome: evidence for impaired development, premature aging, and neurode- generation. Mech Ageing Dev 130: 619–636. doi: 10.1016/j.mad.2009.07.006 PMID: 19647012
7. Natale V (2011) A comprehensive description of the severity groups in Cockayne syndrome. Am J Med Genet 155: 1081–1095.
8. Laine JP, Egly JM (2006) When transcription and repair meet: a complex system. Trends Genet 22: 430–436. doi: 10.1016/j.tig.2006.06.006 PMID: 16797777
9. Bradsher J, Auriol J, Proietti de Santis L, Iben S, Vonesch JL, Grummt I, et al (2002) CSB is a component of RNA pol I transcription. Mol Cell 10: 819–829. PMID: 12419226
10. Yuan X, Feng W, Imhof A, Grummt I, Zhou Y (2007) Activation of RNA polymerase I transcription by cockayne syndrome group B protein and histone methyltrans- ferase G9a. Mol Cell 27: 585–595. doi: 10.1016/j.molcel.2007.06.021 PMID: 17707230
11. Frontini M, Proietti-De-Santis L (2009) Cockayne syndrome B protein (CSB): linking p53, HIF-1 and p300 to robustness, lifespan, cancer and cell fate decisions. Cell Cycle 8: 693–696. doi: 10.4161/cc.8.5.7754 PMID: 19221478
12. Filippi S, Latini P, Frontini M, Palitti F, Egly JM, Proietti-De-Santis L (2008) CSB protein is (a direct target of HIF-1 and) a critical mediator of the hypoxic response. EMBO J 27: 2545–2556. doi: 10.1038/emboj.2008.180 PMID: 18784753
13. Latini P, Frontini M, Caputo M, Gregan J, Cipak L, Filippi S, et al (2011) CSA and CSB proteins interact with p53 and regulate its Mdm2-dependent ubiquitination. Cell Cycle 10: 3719–3730. doi: 10.4161/cc.10.21.17905 PMID: 22032989
14. Frontini M, Proietti-De-Santis L (2012) Interaction between the Cockayne syndrome B and p53 proteins: implications for aging. Aging 4:89–97. doi: 10.18632/aging.100439 PMID: 22383384
15. Caputo M, Frontini M, Velez-Cruz R, Nicolai S, Prantera G, Proietti-De-Santis L (2013) The CSB repair factor is overexpressed in cancer cells, increases apoptotic resistance, and promotes tumor growth. DNA Repair 12: 293–9. doi: 10.1016/j.dnarep.2013.01.008 PMID: 23419237
16. Schröder M, Kaufman RJ (2005) The mammalian unfolded protein response. Annu Rev Biochem 74: 739–89. doi: 10.1146/annurev.biochem.73.011303.074134 PMID: 15952902
17. Schröder M, Kaufman RJ (2006) Divergent roles of IRE1alpha and PERK in the unfolded protein response. Curr Mol Med 6: 5–36. PMID: 16472110
18. Bernales S, Papa FR, Walter P (2006) Intracellular signaling by the unfolded protein response. Annu Rev Cell Dev Biol 22: 487–508. doi: 10.1146/annurev.cellbio.21.122303.120200 PMID: 16822172
19. Marciniak SJ, Yun CY, Oyadomari S, Novoa I, Zhang Y, Jungreis R, Nagata K, Harding HP, Ron D (2004) CHOP induces death by promoting protein synthesis and oxidation in the stressed endoplasmic reticulum. Genes Dev 18: 3066–77. doi: 10.1101/gad.1250704 PMID: 15601821
20. Szegezdi E, Logue SE, Gorman AM, Samali A (2006) Mediators of endoplasmic reticulum stress-induced apoptosis. EMBO Rep 7: 880–5. doi: 10.1038/sj.embor.7400779 PMID: 16953201
21. Mungrue IN, Pagnon J, Kohannim O, Gargalovic PS, Lusis AJ (2009) CHAC1/MGC4504 is a novel proapoptotic component of the unfolded protein response, downstream of the ATF4-ATF3-CHOP cascade. J Immunol 182: 466–76. PMID: 19109178
22. Clarke HJ, Chambers JE, Liniker E, Marciniak SJ. Endoplasmic reticulum stress in malignancy (2014) Cancer Cell 25: 563–73. doi: 10.1016/j.ccr.2014.03.015 PMID: 24823636
23. Carmeliet P, Jain RK (2000) Angiogenesis in cancer and other diseases. Nature 407: 249–57. doi: 10.1038/35025220 PMID: 11001068
24. Tu BP, Weissman JS (2004) Oxidative protein folding in eukaryotes: mechanisms and consequences. J Cell Biol 164: 341–6. doi: 10.1083/jcb.200311055 PMID: 14757749
25. Ma Y, Hendershot LM (2004) The role of the unfolded protein response in tumour development: friend or foe? Nat Rev Cancer 4: 966–77. doi: 10.1038/nrc1505 PMID: 15573118
26. Brunelle JK, Bell EL, Quesada NM, Vercauteren K, Tiranti V, Zeviani M,Scarpulla RC, Chandel NS (2005) Oxygen sensing requires mitochondrial ROS but notoxidative phosphorylation. Cell Metab 1: 409–14. doi: 10.1016/j.cmet.2005.05.002 PMID: 16054090

27. Wang M, Kaufman RJ (2014) The impact of the endoplasmic reticulum protein-folding environment on cancer development. Nat Rev Cancer 14: 581–97. doi: 10.1038/nrc3800 PMID: 25145482

28. Cleaver JE, Brennan-Minnella AM, Swanson RA, Fong KW, Chen J, Chou KM, Chen YW, Revet I, Bezrookove V (2014) Mitochondrial reactive oxygen species are scavenged by Cockayne syndrome B protein in human fibroblasts without nuclear DNA damage. Proc Natl Acad Sci USA 111: 13487–92. doi: 10.1073/pnas.1414135111 PMID: 25136123

29. Guzy RD, Schumacker PT (2006) Oxygen sensing by mitochondria at complex III: the paradox of increased reactive oxygen species during hypoxia. Exp Physiol 91: 807–19. doi: 10.1113/expphysiol.2006.033506 PMID: 16857720

30. Sitia R, Molteni SN (2004) Stress, protein (mis)folding, and signaling: the redoxconnection. Sci STKE 239: pe27.

31. Braakman I, Bulleid NJ (2011) Protein folding and modification in the mammalian endoplasmic reticulum. Annu Rev Biochem 80:71–99. doi: 10.1146/annurev-biochem-062209-093836 PMID: 21495850

32. Groisman R, Kuraoka I, Chevallier O, Gaye N, Magnaldo T, Tanaka K, Kisselev AF, Harel-Bellan A, Nakatani Y (2006) CSA-dependent degradation of CSB by the ubiquitin-proteasome pathway establishes a link between complementation factors of the Cockayne syndrome. Genes Dev 20: 1429–34. doi: 10.1101/gad.378206 PMID: 16751180

33. Nicolai S, Filippi S, Caputo M, Cipak L, Gregan J, Ammerer G, Frontini M, Willems D, Prantera G, Balajee AS, Proietti-De-Santis L (2015) Identification of Novel Proteins Co-Purifying with Cockayne Syndrome Group B (CSB) Reveals Potential Roles for CSB in RNA Metabolism and Chromatin Dynamics. PLoS One 10(6):e0128558. doi: 10.1371/journal.pone.0128558 PMID: 26030138

34. Doyle KM, Kennedy D, Gorman AM, Gupta S, Healy SJ, Samali A (2011) Unfolded proteins and endoplasmic reticulum stress in neurodegenerative disorders. J Cell Mol Med 15: 2025–39. doi: 10.1111/j.1582-4934.2011.01374.x PMID: 21722302

35. Matus S, Glimcher LH, Hetz C (2011) Protein folding stress in neurodegenerative diseases: a glimpse into the ER. Curr Opin Cell Biol 23: 239–52. doi: 10.1016/j.ceb.2011.01.003 PMID: 21288706

36. Huang W, Sherman BT, Lempicki RA (2009) Systematic and integrative analysis of large gene lists using DAVID bioinformatics resources. Nat Protoc 4: 44–57. doi: 10.1038/nprot.2008.211 PMID: 19131956